MOLECULAR IMAGING AND BIOLOGY

Mol Imaging Biol (2018) 20:213–220
DOI: 10.1007/s11307-017-1107-5

Published Online: 24 July 2017

RESEARCH ARTICLE

Comparison of Near-Infrared Imaging Camera Systems for Intracranial Tumor Detection

Steve S. Cho,[1,2] Ryan Zeh,[1] John T. Pierce,[1] Ryan Salinas,[1] Sunil Singhal,[3] John Y. K. Lee[1]

[1]*Department of Neurosurgery, Hospital of the University of Pennsylvania, 235 South Eighth Street, Philadelphia, PA, 19106, USA*
[2]*Perelman School of Medicine at the University of Pennsylvania, Philadelphia, PA, USA*
[3]*Department of Surgery, Hospital of the University of Pennsylvania, Philadelphia, PA, USA*

Abstract

Purpose: Distinguishing neoplasm from normal brain parenchyma intraoperatively is critical for the neurosurgeon. 5-Aminolevulinic acid (5-ALA) has been shown to improve gross total resection and progression-free survival but has limited availability in the USA. Near-infrared (NIR) fluorescence has advantages over visible light fluorescence with greater tissue penetration and reduced background fluorescence. In order to prepare for the increasing number of NIR fluorophores that may be used in molecular imaging trials, we chose to compare a state-of-the-art, neurosurgical microscope (System 1) to one of the commercially available NIR visualization platforms (System 2).

Procedures: Serial dilutions of indocyanine green (ICG) were imaged with both systems in the same environment. Each system's sensitivity and dynamic range for NIR fluorescence were documented and analyzed. In addition, brain tumors from six patients were imaged with both systems and analyzed.

Results: In vitro, System 2 demonstrated greater ICG sensitivity and detection range (System 1 1.5–251 μg/l *versus* System 2 0.99–503 μg/l). Similarly, *in vivo*, System 2 demonstrated signal-to-background ratio (SBR) of 2.6 ± 0.63 before dura opening, 5.0 ± 1.7 after dura opening, and 6.1 ± 1.9 after tumor exposure. In contrast, System 1 could not easily detect ICG fluorescence prior to dura opening with SBR of 1.2 ± 0.15. After the dura was reflected, SBR increased to 1.4 ± 0.19 and upon exposure of the tumor SBR increased to 1.8 ± 0.26.

Conclusion: Dedicated NIR imaging platforms can outperform conventional microscopes in intraoperative NIR detection. Future microscopes with improved NIR detection capabilities could enhance the use of NIR fluorescence to detect neoplasm and improve patient outcome.

Key words: Brain tumor, Comparison, Fluorescence, Imaging, Near-infrared

Introduction

Distinguishing glial tumors from normal brain parenchyma is a critical role for the neurosurgeon during brain tumor surgery. In addition to superb illumination, magnification, and experienced interpretation of color and texture, the neurosurgeon relies on neuronavigation using preoperatively acquired magnetic resonance imaging (MRI) scans and fluorescent dyes. 5-Aminolevulinic acid (5-ALA) has been shown to improve gross total resection rates and progression-free survival in patients with glioblastoma when compared to conventional surgery (without frameless navigation) [1]. However, 5-ALA has limited availability in the USA, and visible light fluorophores suffer from very limited tissue penetration by the fluorescence (on the

Correspondence to: John Lee; *e-mail:* leejohn@uphs.upenn.edu

micron scale) and significant autofluorescence from normal tissue [2]. In contrast, near-infrared (NIR) fluorescent dyes can fluoresce several millimeters through tissue and exhibits virtually no autofluorescence in normal tissue [3]. Indocyanine green (ICG) is the only Food and Drug Administration (FDA)-approved NIR fluorophore (peak excitation at 805 nm) and has been widely used in vascular surgeries [4, 5]. Recently, our group demonstrated that Second-Window-ICG (delayed high dose administration of ICG for tumor visualization) and On-Target-Laboratory 38 (OTL38), a folate analog linked to an ICG-like fluorescent moiety in the same NIR spectrum as ICG, can be systemically injected preoperatively and be used to visualize gliomas, meningiomas, and pituitary adenomas in real time intraoperatively [6–8].

Multiple modalities are commercially available in the operating room suite to detect NIR fluorescence. DSouza et al. systematically reviewed seven fluorescent camera systems and compared their sensitivities and dynamic ranges for NIR fluorophores [9]. Because the operating neurosurgical microscope is critically important to the neurosurgical work flow, and because DSouza et al. did not include conventional neurosurgical microscopes in their analysis, the goal of this study was to compare a conventional neurosurgical microscope with an add-on NIR module against a dedicated near-infrared imaging platform.

Methods

ICG (Akorn Pharmaceuticals, Decatur, IL; $C_{43}H_{47}N_2O_6S_2$-Na) absorbs mainly at 650–900 nm and emits fluorescence at 750–950 nm. It is the only FDA-approved fluorescent drug whose emission lies in the NIR spectrum. We tested visualization of NIR fluorophores in laboratory conditions as well as in the operating room in patients.

Near-Infrared Imaging Systems

The Leica OH6 microscope (Wetzlar, Germany) is one of the conventional neurosurgical microscopes available in the operating room (Fig. 1). The FL800™ module (System 1 henceforth) allows for NIR visualization. The light source is the same xenon light source (emission spectrum in the visible spectrum as well as up to 805 nm in the NIR spectrum) that is used in the visible light range, and its intensity is generally increased to maximum when the FL800 is switched to NIR visualization. A high-sensitivity NIR camera and 820–860-nm filter detect NIR fluorescence and display the image on the monitor in black-and-white [10]. There is no overlay of visible and NIR on the current system. For study purposes, the image was recorded in the provided mp4 format and analyzed offline for analysis. This microscope system will be called System 1 from this point on.

The VisionSense Iridium™ (Philadelphia, PA) is FDA-approved for vascular perfusion imaging in Plastic and Reconstructive and General surgery. The excitation source is a laser tuned in the NIR range (805 nm) with an incident excitation power of 11 mW/cm^2 at 30 cm from tissue. The NIR camera has integrated filters that provide imaging in the NIR range of 820–860 nm. The camera system features a dual optical path design, allowing separate and independent use of white light and near-infrared light. Having separate paths for visible light and NIR images allows very faint fluorescent images to be acquired in the presence of strong white light. The camera system is not integrated into existing microscopes; instead, it is a separate platform with its own light sources for both the visible and NIR spectra (Fig. 1). Image processing was performed in real time and displayed at 1080p video resolution, with recording at 720p. The VisionSense Iridium will be called System 2 from this point on.

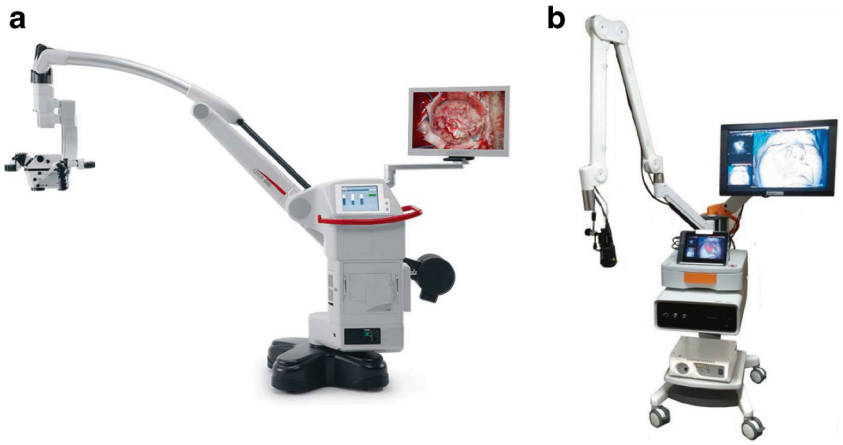

Fig. 1. **a** The Leica OH6 microscope (System 1) is one of the state-of-the-art neurosurgical microscopes with self-balancing, excellent illumination, and magnification through the binocular eyepieces. The Leica FL800 is an add-on NIR imaging module to a pre-existing microscope. **b** VisionSense Iridium™ (System 2), an example of a dedicated near-infrared imaging platform. The tower contains a source of visible light and infrared light and displays the results on the screen with three views (visible light, NIR-overlay, NIR-only) simultaneously. This system does not have oculars and instead all visualization is done on the screen.

Serial Dilutions

Serial dilutions of ICG were prepared in 96-well plates (0.47–1007 μg/l in two-fold dilutions, total of 12 wells) to measure the sensitivity and dynamic range of the two systems in the operating room. The plates were visualized at approximately 25 cm, and the images were recorded and compared. Room testing conditions were equivalent as the two systems were placed side-by-side. All extraneous light sources including windows and overhead lights were eliminated.

Clinical

All patients consented to our IRB-approved study for fluorescent tumor visualization. This prospective cohort study was approved by the University of Pennsylvania Institutional Review Board, and all patients gave informed consent. The trial is registered under clinicaltrials.gov with identifier NCT02280954, and recruitment started in October 2014.

For this study, patients with intracranial brain tumors were injected with 5 mg/kg intravenous injection of ICG as outpatients in a chemotherapy infusion suite approximately 24 hours before surgery based on preclinical studies [11, 12]. The patients were monitored during the infusion and for 30 minutes after infusion with serial vital signs by nurses. There were no immediate complications from ICG administration at this high dose.

Intraoperative Imaging

Patients underwent anesthesia and a craniotomy using anatomic landmarks as well as neuronavigational imaging. Preoperative MRI was used for navigation in all subjects. Three specific views were obtained in order to compare modalities intraoperatively. Upon bone flap removal and after epidural hemostasis had been obtained, a "dura view" was captured with both systems. Upon opening the dura and reflecting the dura back, a "cortex view" was obtained. After corticectomy had been performed and the tumor had been exposed, another "tumor view" was obtained. Surgery then proceeded in the standard manner without the use of NIR imaging adjuncts. If the NIR signal was not identified before corticectomy, an additional attempt was made at the time of tumor identification. The rest of the surgery proceeded as per our protocol in the SWIG (Second Window ICG) study.

Patients were admitted to the intensive care unit following surgery. There were no adverse outcomes. A postoperative MRI took place on the first postoperative day. Patients were seen at approximately 2 and 4 weeks from surgery.

Image Acquisition and Analysis

For both the 96-well plates and the human patients, NIR signal was visualized using both Systems 1 and 2. Any time NIR imaging was performed, all ambient light was shut off, and window shades were completely closed in an effort to minimize stray NIR light. Image analysis and signal-to-background ratio (SBR) calculations were conducted using ImageJ software (https://imagej.nih.gov) by taking three to five regions of interest points on the fluorescent area and an equal number of points on the background area.

Statistical Analysis

Statistical comparison of Systems 1 and 2 was performed using *t* tests, calculated using the GraphPad QuickCalcs software (https://www.graphpad.com/quickcalcs/ttest1.cfm).

Results

Serial Dilution Comparison

The two systems were compared using identical serial dilutions of ICG (Fig. 2). System 1 was able to detect ICG concentrations ranging 1.5–251 μg/l, with peak detection at 31.0–62.0 μg/l with SBR of 3.25. System 2 was able to detect a range of 0.99–503 μg/l, with peak detection at 7.7–62.0 μg/l with SBR of 12, the maximum SBR for the camera. Of note, both systems' fluorescence detection decreased at concentrations higher than 62.0 μg/l, due to an auto-quenching phenomenon that occurs when highly concentrated fluorophores absorb photons from neighboring fluorophores, reducing overall measurable signal. At all ICG concentrations, the signal strength was both qualitatively and quantitatively superior with System 2.

Comparison of Intraoperative NIR Visualization

Of the patients enrolled in the SWIG study, six patients had imaging performed with both camera systems (Table 1). Subjects had an age range from 39 to 67. Four subjects were male. Histology included two glioblastomas, two brain metastases, one hemangioblastoma, and one meningioma.

We compared the imaging acquired with the two camera systems in all six patients. Figure 3 shows images in one example patient, and Fig. 4 shows the overall data. With the dura intact, all six tumors were not visible to the surgeon under white light (Fig. 3c, first column). Since near-infrared can penetrate normal tissue up to approximately 1 cm, we hypothesized that we may be able to see the NIR signal through the dura. Using System 1, the NIR fluorescence SBR was measured to be 1.2 ± 0.15. In contrast, System 2 provided a SBR of 2.6 ± 0.63. The SBR was significantly higher using System 2 (*t* test, $p = 0.0051$). Hence, System 2 allowed for localization of tumor even through the dura prior to dural opening.

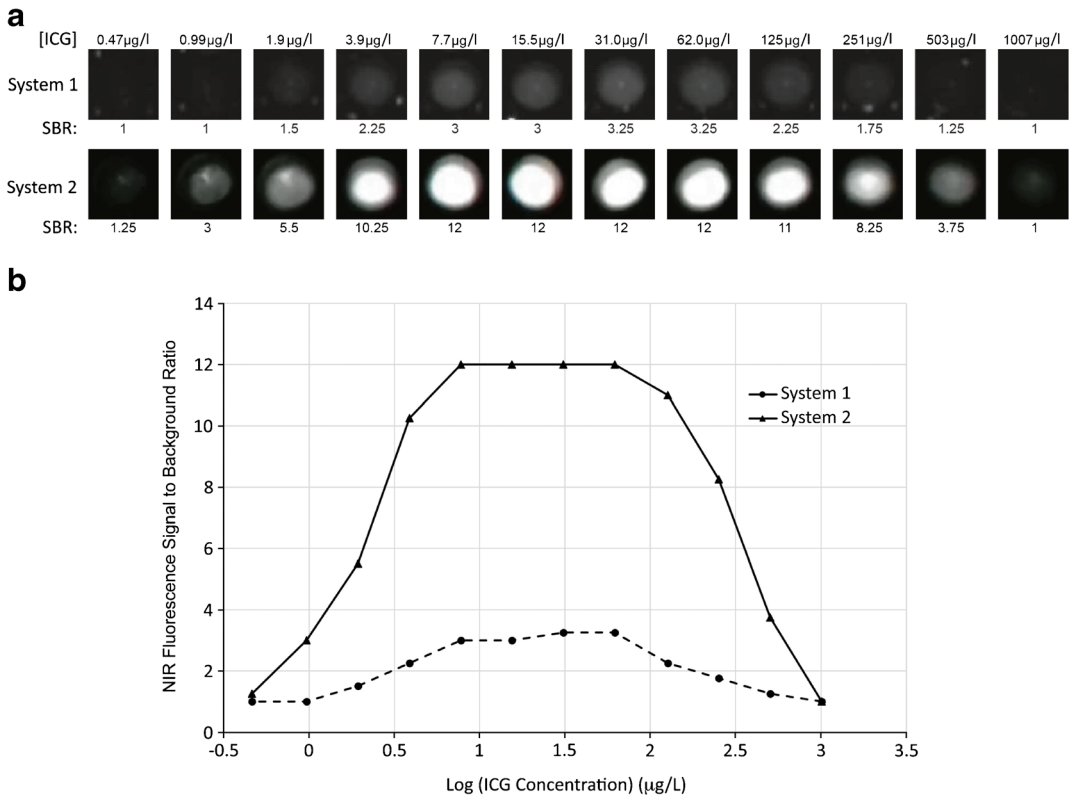

Fig. 2. Comparing NIR sensitivity of a dedicated NIR detector and an add-on detector to pre-existing microscope. **a** Serial dilutions of ICG ranging from 0.47 to 1007 μg/l. The same plates were imaged using System 1 and System 2. Below each well is the signal-to-background ratio of the corresponding well in the respective visualization systems. An SBR = 1 shows that the fluorescence signal is the same as background = *black*. **b** Plot of SBR *versus* log concentration ranging from 0.47 to 1007 μg/l. the SBR peaks near 3 for System 1 and 12 for System 2. At concentrations above 62.0 μg/l, there is auto-quenching of the fluorophores.

After the dura was opened, the tumor was at least partially visualized under white light in two patients with meningiomas but not in other patients. The NIR fluorescence SBR was 1.4 ± 0.19 for System 1 and 5.0 ± 1.7 for System 2 (*t* test, $p = 0.0026$). Thus, in many cases, even if the tumor was not visible with white light, the NIR systems could provide faint (System 1) and moderate (System 2) NIR signal through normal brain parenchyma.

Finally, after corticectomy and upon tumor exposure, the tumor was detectable by visible light in all six cases. The NIR SBR was 1.8 ± 0.26 for System 1 and 6.1 ± 1.9 for System 2 (*t* test; $p = 0.0013$). As can be seen in Figs. 3 and 4, the SBR was superior in all cases using System 2 *versus* System 1.

Based on this analysis, System 1 was able to visualize ICG accumulation utilizing the Second Window ICG technique, but it demonstrated relatively strong signal only after corticectomy when the neoplastic tissue was in direct line of sight. Conversely, System 2 detected fluorescence with strong SBR through normal brain parenchyma and even through the dura in select cases (see Fig. 3 for example).

Discussion

The majority of neurosurgical experience for fluorescent tumor visualization is with the visible light fluorescent prodrug 5-ALA [1, 13, 14]. Near-infrared dyes have been

Table 1. Patient information, tumor location, pathology, and ICG signal strength upon tumor exposure

Patient ID	Sex	Age	Tumor type	Tumor Location	SBR (System 1)	SBR (System 2)
ICG75	Male	67	Glioblastoma multiforme	Right occipital lobe	2.2	4.2
ICG92	Male	65	Glioblastoma multiforme	Left temporal lobe	1.9	5.2
ICG78	Female	52	Breast cancer metastasis	Right frontal lobe	1.8	8.5
ICG85	Male	60	Lung cancer metastasis	Left frontal lobe	1.7	N/A[a]
ICG70	Male	39	Hemangioblastoma	Left cerebellum	1.6	3.9
ICG88	Female	43	Meningioma	Anterior cranial fossa	1.5	6.4

[a]System 2 scope was unavailable

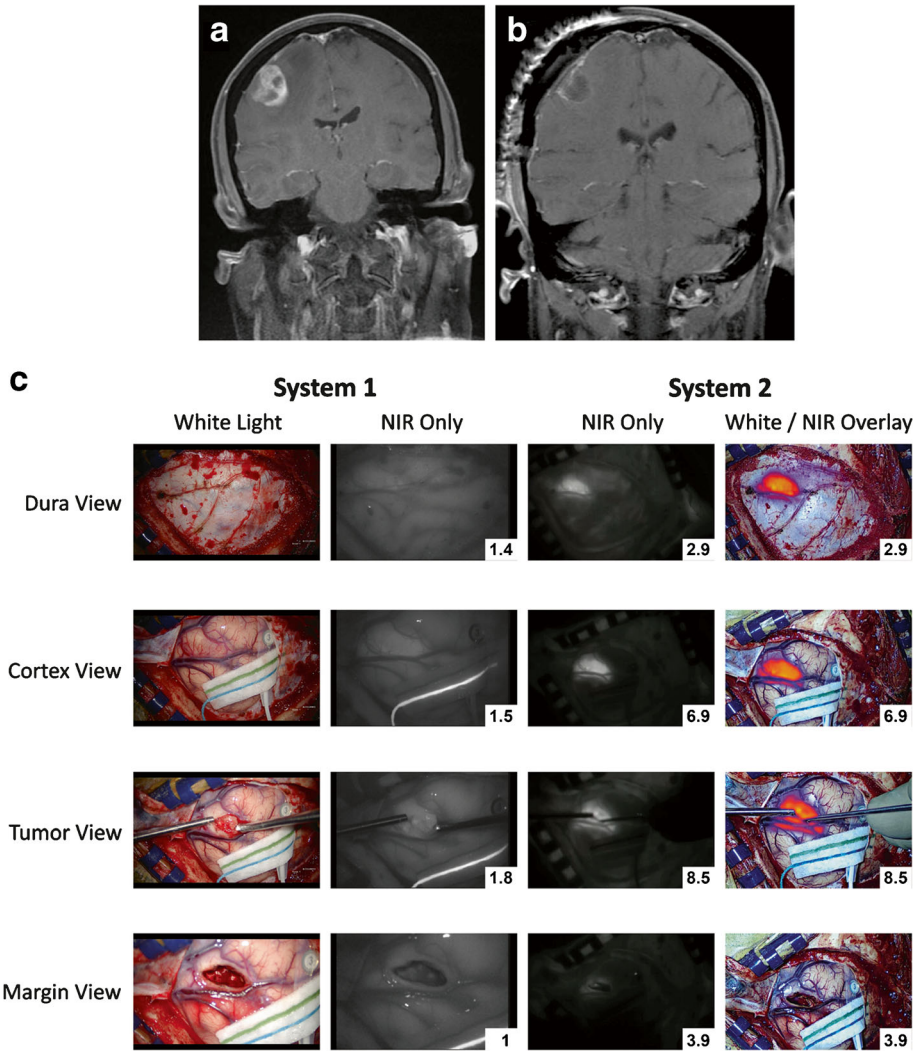

Fig. 3. Comparison of System 1 and System 2 in a patient with breast cancer metastasis to the brain. **a** Preoperative and **b** postoperative coronal T1 MRI with contrast showing metastasis and resection in the right frontal lobe. **c** Images comparing Systems 1 and 2 at four different times during the surgery. The *top row* shows the view with the dura intact—dura view. The *second row* shows the view with the dura open but the cortex intact—cortex view. The *third row* shows the view with the tumor exposed after corticectomy—tumor view. The *last row* shows the view after resection of tumor—margin view. The *first column* on the left shows the visible light view only with System 1. The *second column* shows the NIR view (*black/white*) of System 1. Notice that the background normal brain appears to be almost as bright as the tumor itself in the tumor view row, thus accounting for the relatively low SBR of System 1. The *third column* shows the NIR view (*black/white*) of System 2. Notice that the background normal brain appears to be quite dark or absent of NIR signal. The *fourth column* shows the pseudocolor overlay with NIR superimposed on the visible light view. This view is projected in real time by System 2.

used for videoangiography, but its use in fluorescent tumor visualization is novel [4, 5, 15, 16]. NIR dyes have great promise given their increased tissue penetration and lack of normal brain autofluorescence. Our recently described technique—Second Window ICG—provides a means of administering an FDA-approved drug, ICG, in higher concentrations than usual (5 mg/kg *versus* the usual dose of 0.3 mg/kg) and in a delayed fashion (approximately 24 h prior to surgery *versus* seconds before for angiography) to allow sensitive visualization of gliomas and meningiomas [6, 8]. As the dye is cleared from normal brain parenchyma, sufficient ICG remains in abnormal tumor tissue due to the enhanced permeability and retention effect, thus allowing for tumor localization and identification [17]. Furthermore, we recently demonstrated that a systemic injection of OTL38, a folate analog linked to ICG, preoperatively allows visualization of pituitary adenomas [7]. Likewise, there are many novel dyes that are being conjugated to ICG, ICG-like drugs, or IRDye800 (LiCor). These dyes all fluoresce in the near-infrared range, and thus a proper study of camera systems for near-infrared visualization is paramount.

Because of this increased interest in NIR fluorescent dyes, DSouza et al. reviewed several dedicated fluorescent tumor optical imaging platforms, but this study did not

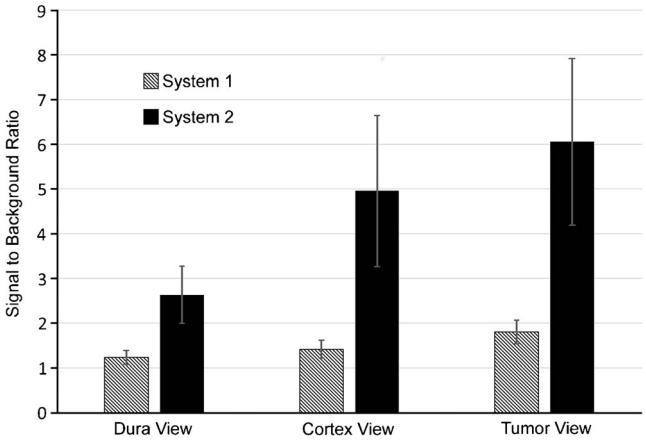

Fig. 4. Detection of NIR signal from tumor through intact dura, through cortex, or direct tumor view using Systems 1 and 2. In all three views, System 2 demonstrates significantly higher signal-to-background ratios (*t* test, $p = 0.0051$, 0.0026, 0.0013, respectively).

include neurosurgical microscopes [9]. The Leica OH6 with FL800™ (System 1) is a commonly used visualization platform for neurosurgical procedures. In contrast, VisionSense Iridium™ (System 2) is a dedicated NIR imaging platform not commonly used in neurosurgery at present. Each modality has its advantages and disadvantages. The ideal imaging modality would be sensitive to NIR signals, be able to overlay real-time fluorescence on white light images, and be operable with minimal additional effort and time.

Comparison of the Two Systems

Our comparison of these two camera systems for visualizing NIR fluorescence demonstrates that the dedicated platform (System 2) can outperform existing neurosurgical microscopes in terms of sensitivity and dynamic range (Figs. 2, 3, and 4). One possible reason for the difference in sensitivity lies in the excitation source for NIR fluorophores. Conventional neurosurgical microscopes simply use existing light sources and, despite maximal intensity, the amount of power in the NIR range may not be sufficient. Conversely, a dedicated NIR visualization platform is capable of having its own laser output source that is tuned to the NIR range, resulting in much stronger excitation output, ultimately leading to higher NIR sensitivity. This is detailed in Fig. 5.

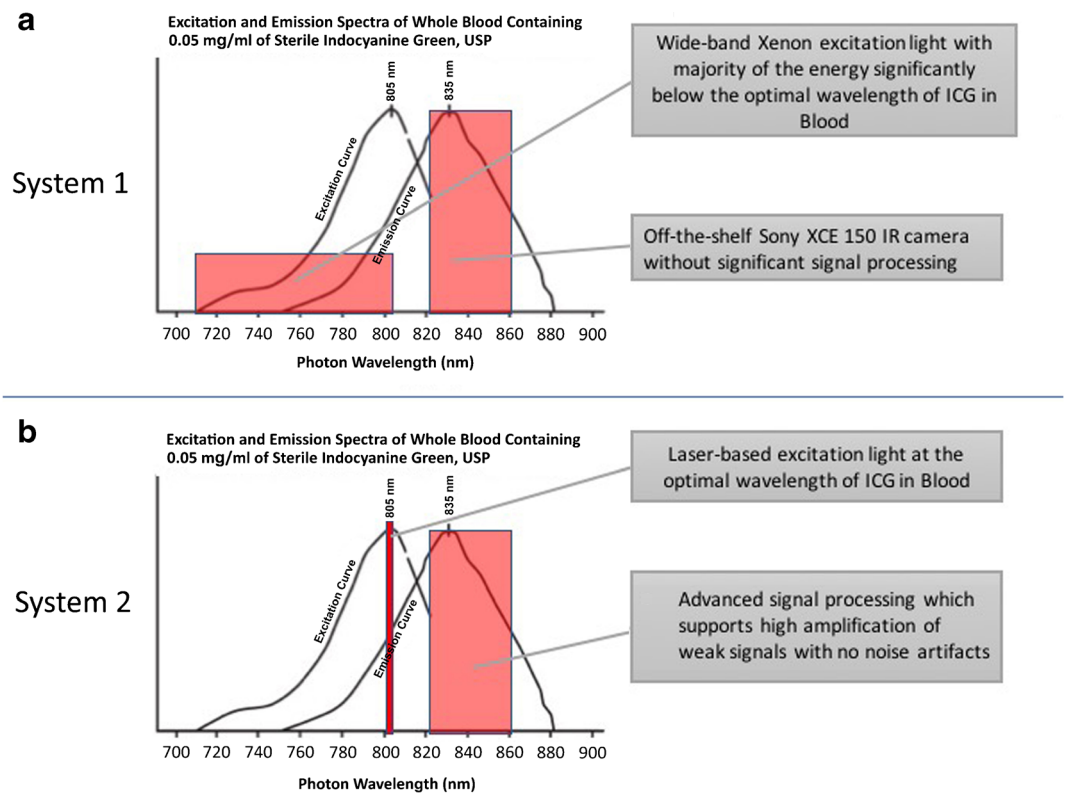

Fig. 5. Comparison of ICG visualization technology utilized by System 1 and System 2. **a** System 1 utilizes a Xenon light source, which emits photos in the visible light range as well as in the NIR range. The majority of the energy is below the optimal wavelength of ICG in blood (805 nm). Emission from ICG is detected by a camera with filters for maximum emission spectrum of ICG in blood at 820–860 nm but without significant signal processing [10]. **b** System 2 utilizes a laser-based excitation light source, which is tuned to 805 nm, the optimal wavelength of ICG in blood. Furthermore, the NIR camera is tuned to capture the maximum emission spectrum of ICG in blood at 820–860 nm and has advanced signal processing that supports amplification of weak signals.

Another advantage of the dedicated near-infrared camera system is the ability to see real-time overlay of the NIR signal on visible light image (Fig. 3c, column 4). This is made possible by the dual optical path design used in System 2, as well as the dedicated camera system that integrates information from both paths to overlay the images. This overlay allows for more natural image appreciation during surgery, albeit only in two dimensions. In contrast, the microscope-based NIR system requires the surgeon to look at the 2-D image in black-and-white only (Fig. 3c, column 2). This limited information can make localization of NIR signal difficult.

In addition, to these obvious differences, there appear to be many other differences between the systems that cannot easily be tested. For example, optics in the microscope may have different coatings that differentially allow NIR to pass through each stage of the lens in microscope systems. In contrast, dedicated NIR systems appear to have less optics through which the NIR signal must pass to reach the sensor, and thus this may differentially affect sensitivity. In addition, the choice of sensor may be critical in that NIR sensitivity may be different between the sensors. Indeed, DSouza et al. discuss at length the advantages of high bit depth (12 to 16 bit) *versus* low bit (8 bit) in the ability of different sensors to extract NIR light information. Additionally, computer processing of this sensor information may vary among systems, and in fact, DSouza et al. comment that the VisionSense system provides high bit depth as well as excellent software algorithms to extract this information [9]. All of these issues may contribute to differences in NIR sensitivity.

Despite the advantages of dedicated NIR imaging platforms (System 2), neurosurgeons are accustomed to using microscopes (System 1) in their operative workflow. Presently, dedicated NIR imaging platforms exist as separate towers and they must be brought into the operating field whenever imaging is performed. Each time the scope is employed, time is added to the operation due to the various machines that must be moved in a careful and sterile manner. In addition, the ergonomics change as the neurosurgeon has to look at the video screen rather than the oculars of the microscope. Finally, the microscope has a distinct advantage over the dedicated platform in its high magnification, which is crucial for neurosurgeons.

Future Directions

Recently, neurosurgical microscope companies have introduced modules that allow for direct injection of the digital image into the optic image of the eyepiece, but image overlay of the NIR onto the visible image is still unavailable. Ultimately, what neurosurgeons will need is a dedicated NIR imaging system that can easily be integrated into existing neurosurgical microscopes. This will obviate the need for two separate platforms and the associated additional time and space. For such a system, having two light sources, one for normal white light and one dedicated to NIR imaging, as well a dual optical path design will be crucial in capturing relatively faint NIR signals in the presence of strong white light. Work is already in progress, such as the Dual-Image VideoAngiography (DIVA) developed by Sato et al., which was "designed to provide dual high-resolution images from an operating microscope as a single image on a large monitor" [18]. Further work in this direction, including using laser excitation sources, will facilitate the use and research of NIR fluorophores in the operating room, ultimately leading to enhanced tumor resection rates and decreased patient mortality.

Limitations

This study is limited by the study of only one NIR fluorophore, ICG. In addition, the sample size was only six patients. Another limitation of this study is the inclusion of only the Leica microscope and the VisionSense Iridium^{TM}. It would have been useful to include the Zeiss microscope as well as other camera systems such as SurgVision. Despite these limitations, we believe this paper points to some of the challenges and future opportunities in near-infrared imaging.

Conclusion

This study compared two imaging modalities for near-infrared fluorescence for use in the operating room for real-time visualization of intracranial neoplastic tissue. Our results suggest that a dedicated NIR visualization platform outperforms add-on modules to traditional microscopes, both in terms of sensitivity to fluorescence and dynamic range of detection. While current dedicated platforms add to operation duration and limited floor space in the operating room, future microscopes with improved NIR detection capabilities could enhance the use of NIR fluorescence to detect neoplasm and improve gross total resection and patient outcome.

Acknowledgements. Thank you to Jun Jeon, a medical student at the Perelman School of Medicine, for helping with the Figures.

Compliance with Ethical Standards

Funding

This work was partially supported by the National Institutes of Health R01 CA193556 (SS) and the Institute for Translational Medicine and Therapeutics of the Perelman School of Medicine at the University of Pennsylvania (JYKL). In addition, research reported in this publication was supported by the National Center for Advancing Translational Sciences of the National Institutes of Health under Award Number UL1TR000003 (JKYL). The content is solely the responsibility of the authors and does not necessarily represent the official views of the NIH.

Conflict of Interest

JYKL owns stock options in VisionSense™. SS holds patent rights over technologies presented in this manuscript.

References

1. Stummer W, Pichlmeier U, Meinel T et al (2006) Fluorescence-guided surgery with 5-aminolevulinic acid for resection of malignant glioma: a randomised controlled multicentre phase III trial. Lancet Oncol 7:392–401
2. Koizumi N, Harada Y, Minamikawa T et al (2016) Recent advances in photodynamic diagnosis of gastric cancer using 5-aminolevulinic acid. World J Gastroenterol 22:1289–1296
3. Frangioni JV (2003) *In vivo* near-infrared fluorescence imaging. Curr Opin Chem Biol 7:626–634
4. Lavazza M, Liu X, Wu C et al (2016) Indocyanine green-enhanced fluorescence for assessing parathyroid perfusion during thyroidectomy. Gland Surg 5:512–521
5. Yeoh MS, Kim DD, Ghali GE (2013) Fluorescence angiography in the assessment of flap perfusion and vitality. Oral Maxillofacial Surg Clinics North Am 25:61–66
6. Lee JYK, Pierce J, Thawani JP et al (2017) Near-infrared fluorescent image-guided surgery for intracranial meningioma. J Neurosurg 7:1–11
7. Lee JYK, Cho SS, Zeh R et al (2017) Folate receptor overexpression can be visualized in real time during pituitary adenoma endoscopic transsphenoidal surgery with near-infrared imaging. J Neurosurg. doi:10.3171/2017.2.JNS163191
8. Lee JYK, Thawani JP, Pierce J et al (2016) Intraoperative near-infrared optical imaging can localize gadolinium-enhancing gliomas during surgery. Neurosurgery 79:856–871
9. DSouza AV, Lin H, Henderson ER et al (2016) Review of fluorescence guided surgery systems: identification of key performance capabilities beyond indocyanine green imaging. J Biomed Opt 21(8):80901
10. Sturgis M. (2006) Section 5. 510(k) summary for Leica FL800, submitted to the Food and Drug Administration, Division of General, Restorative and Neurological Devices
11. Madajewski B, Judy BF, Mouchli A et al (2012) Intraoperative near-infrared imaging of surgical wounds after tumor resections can detect residual disease. Clin Cancer Res 18:5741–5751
12. Jiang JX, Keating JJ, Jesus EM et al (2015) Optimization of the enhanced permeability and retention effect for near-infrared imaging of solid tumors with indocyanine green. Am J Nucl Med Mol Imaging 5:390–400
13. Colditz MJ, van Leyen K, Jeffree RL (2012) Aminolevulinic acid (ALA)–protoporphyrin IX fluorescence guided tumour resection. Part 2: theoretical, biochemical and practical aspects. J Clin Neurosci 19:1611–1616
14. Colditz MJ, Jeffree RL (2012) Aminolevulinic acid (ALA)–protoporphyrin IX fluorescence guided tumour resection. Part 1: clinical, radiological and pathological studies. J Clin Neurosci 19:1471–1474
15. Gossedge G, Vallance A, Jayne D (2015) Diverse applications for near infra-red intraoperative imaging. Color Dis 17:7–11
16. Ewelt C, Nemes A, Senner V et al (2015) Fluorescence in neurosurgery: its diagnostic and therapeutic use. Rev Lit J Photochem Photobiol B: Biol 148:302–309
17. Iyer AK, Khaled G, Fang J, Maeda H (2006) Exploiting the enhanced permeability and retention effect for tumor targeting. Drug Discov Today 11:812–818
18. Sato T, Suzuki K, Sakuma J et al (2015) Development of a new high-resolution intraoperative imaging system (dual-image videoangiography, DIVA) to simultaneously visualize light and near-infrared fluorescence images of indocyanine green angiography. Acta Neurochir 157:1295–1301